Cell Replacement in Human Lung Bioengineering

Brandon A. Guenthart MD , John D. O'Neill PhD , Jinho Kim PhD , Kenmond Fung CCP , Gordana Vunjak-Novakovic PhD , Matthew Bacchetta MD

PII: S1053-2498(18)31743-1
DOI: https://doi.org/10.1016/j.healun.2018.11.007
Reference: HEALUN 6850

To appear in: *Journal of Heart and Lung Transplantation*

Please cite this article as: Brandon A. Guenthart MD , John D. O'Neill PhD , Jinho Kim PhD , Kenmond Fung CCP , Gordana Vunjak-Novakovic PhD , Matthew Bacchetta MD , Cell Replacement in Human Lung Bioengineering, *Journal of Heart and Lung Transplantation* (2018), doi: https://doi.org/10.1016/j.healun.2018.11.007

Cell Replacement in Human Lung Bioengineering

Brandon A. Guenthart MD[1,2], John D. O'Neill PhD[2], Jinho Kim PhD[2,3], Kenmond Fung CCP[4], Gordana Vunjak-Novakovic PhD[2,5], and Matthew Bacchetta MD[1*]

[1]Department of Surgery, Columbia University Medical Center, Columbia University, New York, New York 10032, USA. [2]Department of Biomedical Engineering, Columbia University Medical Center, Columbia University, New York, New York 10032, USA. [3]Department of Biomedical Engineering, Stevens Institute of Technology, Hoboken, NJ. [4]Department of Clinical Perfusion, Columbia University Medical Center, Columbia University, New York, NY 10032, USA. [5]Department of Medicine, Columbia University Medical Center, Columbia University, New York, New York 10032, USA. 10032, USA. *email: matthew.bacchetta@vanderbilt.edu

Corresponding Author:

Matthew Bacchetta, MD, MBA, MA

Department of Thoracic Surgery

Vanderbilt University Medical Center

609 Oxford House

1313 21st Ave South

Nashville, TN 37232

Phone: (212) 305-3408

Email: matthew.bacchetta@vanderbilt.edu

Abstract

Background: As the number of patients with end-stage lung disease continues to rise, there is a growing need to increase the limited number of lungs available for transplantation. Unfortunately, attempts at engineering functional lung *de novo* have been unsuccessful, and artificial mechanical devices have limited utility as a bridge to transplant. This difficulty is largely due to the size and inherent complexity of the lung; however, recent advances in cell-based therapeutics offer a unique opportunity to enhance traditional tissue engineering approaches with targeted site- and cell-specific strategies.

Methods: Human lungs deemed unsuitable for transplantation were procured and supported using novel cannulation techniques and modified *ex vivo* lung perfusion. Targeted lung regions were treated using intratracheal delivery of decellularization solution. Labeled mesenchymal stem cells or airway epithelial cells were then delivered into the lung and incubated for up to 6 hours.

Results: Tissue samples were collected at regular time intervals and detailed histologic and immunohistochemical analyses were performed to evaluate the effectiveness of native cell removal and exogenous cell replacement. Regional decellularization resulted in the removal of airway epithelium with preservation of vascular endothelium and extracellular matrix proteins. Following incubation, delivered cells were retained in the lung and showed homogeneous topographic distribution and flattened cellular morphology.

Conclusions: Our findings suggest that targeted cell replacement in extracorporeal organs is feasible and may ultimately lead to chimeric organs suitable for transplantation or the development of *in situ* interventions to treat or reverse disease, ultimately negating the need for transplantation.

Introduction

The growing need for transplantable organs continues to drive development and expand the capabilities of tissue engineering and regenerative medicine. The need for a viable alternative to traditional donor organ utilization is perhaps most evident in the field of lung transplantation. For thousands of patients with end-stage lung disease, transplantation remains the only option. Despite efforts to expand the donor organ pool(1-3), the number of lung transplantations performed annually has not risen significantly, and wait list mortality continues to rise(4).

Recapitulating the complexity of the lung and bioengineering functional tissue capable of gas exchange is challenging. Historically, biomedical engineers have approached this problem from two directions: (**i**) Bottom-up (or modular) approach, involving the formation of a bioinspired microarchitectural unit (e.g., the alveolus), which when scaled can form complex tissues capable of organ-specific function. The lung, however, has over 40 distinct cell types(5) and multiple tissue types with region-specific composition and function. It is estimated that one cubic millimeter of lung parenchyma contains more than 170 alveoli(6). Given the size and anatomical complexity of a human lung, this approach may be best suited for *in vitro* microsystems (e.g., organ-on-a-chip) and have little practical application in whole organ bioengineering. (**ii**) Top-down approach, involving recellularization strategies using biodegradable, artificial, or decellularized biomimetic scaffolds. In 2010 whole organ perfusion-based decellularization was reported in rodent models(7, 8). Although these studies, and subsequent scaled studies using porcine and human lungs(9, 10), served as proofs-of-concept that decellularized scaffolds could support the engraftment of various cell types, transplanted lung constructs failed within hours due to severe pulmonary edema and micro emboli within the pulmonary vasculature. As progress with this approach has been limited, further investigations are needed to identify appropriate cell populations and dosages capable of

regeneration, to optimize delivery strategies, and to develop more robust bioreactor systems for whole organ culture.

Currently, there is considerable interest in investigating cell-based therapeutics to ameliorate lung injury or treat disease. Mesenchymal stem cells (MSC) have been shown to augment injury recovery through paracrine activity(11-13) and mitochondrial transfer(14), and their use is currently under investigation in a number of human clinical trials. Additionally, investigators have explored the use of pluripotent cells, which have tremendous potential in treating or reversing the course of lung disease and in bioengineering new lung tissue. Following the landmark discovery of induced pluripotent stem cells (iPSC) in 2006 by Yamanaka and colleagues(15), there has been tremendous interest in autologous cell therapy. Somatic reprogramming and genetic manipulation offers the ability to produce an unlimited supply of healthy patient-specific progenitor cells. In the case of lung disease, these cells have the potential to be used in cell replacement therapy, a process involving the removal of diseased or damaged cells and subsequent replacement with healthy progenitors. As seen with hematopoietic cell-based therapies, even low levels of chimerism can effectively reverse disease phenotype(16, 17). Similar evidence suggests that a correction of only 5 – 10% of the airway epithelial cells in patients with cystic fibrosis may restore normal chloride secretion(18, 19).

Here, we assessed the potential for targeted cell removal and cell replacement therapy using human lungs unacceptable for transplantation and supported with *ex vivo* lung perfusion (EVLP) (**Fig. 1A**). Additionally, to explore the clinical potential of our approach, we further characterized unacceptable human lungs and detailed our EVLP setup, cannulation techniques, and novel transpleural imaging system for the *in-situ* visualization of delivered cells in real time. Our data

demonstrate that regional decellularization followed by recellularization using controlled micro-volume delivery techniques(20) in predetermined lung regions resulted in: (**i**) the selective removal of pulmonary epithelium, (**ii**) the maintenance of native lung architecture and retention of essential extracellular matrix components, and (**iii**) the efficient delivery, topographic distribution, and attachment of therapeutic cells into targeted lung segments.

Methods

Human lung procurement – To demonstrate the utility of our methods in a clinically relevant model, we procured human lungs deemed unacceptable for transplant. Lungs were harvested in standard clinical fashion(21, 22) from donors following brain death. The use of human tissue for research received a waiver from the Institutional Review Board (IRB) at Columbia University and approval from LiveOnNY organ donor network.

Characterization of donors with lungs deemed unsuitable for transplantation – A comprehensive review was conducted to identify the literature published worldwide describing donor characteristics in cases where lungs were deemed unsuitable for transplantation. Analysis only included lungs donated after brain death with no warm ischemic time and excluded donors suffering from cardiac death. Pooled data are reported as mean ± standard deviation or as *n* (%).

Lung cannulation – The aortic arch, pericardium, or another large donor vessel was connected to the left atrial cuff with a running 6-0 prolene suture (Ethicon), and a custom 36 F crenellated venous drainage cannula was secured in place with a 2-0 Ti-Cron tie (Covidien). The use of a "bio-

bridge" was adapted from previously described methods in a porcine model(23). An 18 – 20 F pulmonary artery cannula was secured in place with a purse-string 5-0 prolene suture, and the trachea was cannulated with a 7.5 mm cuffed endotracheal tube (Sheridan).

Ex vivo lung perfusion – A double-lined organ basin heated with a recirculating warm saline circuit was placed in the preservation chamber (XVIVO), equipped with a humidification system and ambient temperature controls. Lungs were placed in prone position, and the cannulas were secured. EVLP technique was based on previously described methods(24). Thermal images of the lung were captured using a FLIR T430sc infrared camera (FLIR Systems Inc.) EVLP was conducted for up to 6 hrs.

Regional decellularization – Decellularization of target lung regions was achieved by intratracheal delivery of decellularization solution. A mild detergent solution previously described(25), containing 8 mM 3-[(3-Cholamidopropyl)dimethylammonio]-1-propanesulfonate (CHAPS), 0.5 M NaCl, and 25 mM ethylenediaminetetraacetic acid (EDTA) was introduced bronchoscopically into targeted bronchopulmonary segments by a custom micro-catheter delivery system. Immediately following withdrawal of the bronchoscope, a 4 – 7 F Fogarty occlusion catheter (Edwards Lifesciences) was inflated and left in place to prevent escape of decellularization fluid from the targeted region. Decellularization solution was allowed to dwell for 1 hour, and was then replaced with fresh solution for an additional 1 hour before repeated bronchoalveolar lavage with sterile normal saline. During airway decellularization, the vascular compartment remained perfused and in native condition (i.e., did not undergo decellularization). To assess the effectiveness of decellularization, lung wedge samples were collected following decellularization and prior to further intervention, fixed, embedded, de-paraffinized, and imaged, as previously described.

Therapeutic cell delivery – Cell delivery was performed using a 3.8 mm flexible bronchoscope with a 1.2 mm lumen for therapeutic delivery and intervention. Mesenchymal stem cells or airway epithelial cells labeled with carboxyfluorescein succinimidyl ester (CFSE) were delivered locally into targeted lobes or segments. Subsequent live transpleural imaging of near infrared-labeled cells was performed using a custom imaging system developed in our lab and consisting of LED excitation source (M780L3, Thorlabs), camera (Zyla 4.2, Andor Technology Co.), and objective (Plan N 10×, Olympus)(23). To assess the distribution and evidence of early engraftment of delivered cells, lung wedge samples were collected at the conclusion of the experiment, fixed, embedded, de-paraffinized, and imaged, as previously described.

See online data supplement for additional methods.

Results

Human Lung *Ex Vivo* Perfusion

Lungs deemed unsuitable for transplantation were procured in standard fashion from donors following brain death (n = 6). An EVLP platform with integrated circuit elements was developed and used to provide *ex vivo* lungs 6 hours of normothermic perfusion (**Fig. 2A,B**). The procedure for cannulation and management of pulmonary venous drainage is outlined in **Fig. 3A**. A donor vessel (e.g., aortic arch) or tissue (e.g., pericardium) was used as a natural bio-bridge to facilitate cannulation of the pulmonary veins (PV) (**Fig. 3B**). Next, the pulmonary artery (PA) and trachea were cannulated (**Fig. 3A, iii**). Target parameters for extracorporeal lung perfusion and ventilation

were: PA pressure, < 20 mmHg; PV pressure, 3 – 5 mmHg; flow, 0.2 – 0.4 L/min, temperature, 36 – 38 °C; respiratory rate, 6 – 8 bpm; tidal volume, 6 mL/kg; fraction of inspired oxygen (FiO_2), 40%. Real-time monitoring and feedback-regulated pressure-limited control allowed for tight regulation of vascular flow (**Fig. 2C**). Adjustments in the height differential between the lung and perfusate reservoir allowed for modulation of hydrostatic pressure and precise maintenance of the trans-pulmonary pressure gradient (**Fig. 2D**).

Donor and Lung Characteristics

Representative imaging prior to procurement demonstrated lobar collapse and consolidation on computed tomography (CT) scan (**Fig. 3C, i**) and opacities/atelectasis on chest X-ray (CXR) (**Fig. 3C, ii**). Gross imaging of donor lungs highlighted lung regions which were not able to be recruited (i.e., ventilated) during the procurement process (**Fig. 3C, iii, iv**). Bronchoscopy demonstrated inflammation and thick copious secretions in the airways (**Fig. 3C, v, vi**), and PAS staining of BAL specimens demonstrated abundant cellular content (**Fig. 3E**). Thermography showed lungs efficiently cooled and placed in the warm organ basin following flush and cannulation (**Fig. 3D**). At the start of EVLP, a fluorescent cell viability marker (CSFE) was delivered to the distal lung, where uptake of CFSE confirmed cell viability (**Fig. 3F**).

To better understand and characterize lungs deemed unsuitable for transplantation, a comprehensive literature review was conducted. Data was combined from previous reports of brain death donors whose lungs were unable to be used for transplantation(26-43) (**Table 1**). Donor age was 45.7 ± 6.9 years on average, and 59.8% of donors were male. Trauma was the leading cause of brain death (56.8%), followed by intracerebral hemorrhage (34.2%) and other causes such as cardiac arrest with return of spontaneous circulation (ROSC) or ischemic brain

injury (8.9%). Of those reported, 23.1% of lungs had a significant smoking history (> 20 pack years), and 6.9% had an underlying pulmonary disease (e.g., asthma, pulmonary hypertension, emphysema). Lungs on average had a PaO_2/FiO_2 ratio of 259.18 ± 66.92 mmHg, and an abnormal CXR or suspected pneumonia/infection was present in 36.5% and 26.5% of cases, respectively.

Human Lung Decellularization

To demonstrate the ability to selectively remove airway epithelium (**Fig. 4A**), targeted lobes or bronchopulmonary segments were decellularized by micro-catheter delivery of a decellularization solution (CHAPS)(25). Blue dye was added to allow for bronchoscopic and gross visualization of the treated area (**Fig. 4B**). Histologic analysis by hematoxylin and eosin staining (H&E) demonstrated native lung with intact respiratory epithelium (**Fig. 4C, i-iii**) and treated lung with loss of nuclear staining in distal alveoli and removal of epithelium in large airways (**Fig. 4C, iv-vi; Sup. Fig 1A**). Transmission electron microscopy (TEM) showed native lung covered by type I pneumocyte cell membranes and a healthy type II pneumocyte (arrow). Following decellularization, TEM revealed the removal of type I pneumocytes and exposed basement membrane on either side of the blood gas barrier. In **Fig. 4D** (right), a preserved endothelial cell (star) is shown within a capillary adjacent to an injured type II cell (arrow) detaching from the basement membrane. Trichrome staining of the lung demonstrated retention of extracellular matrix components including collagen and elastic fibers (**Fig. 4E, i,ii**), silver stain demonstrated preservation of reticular fibers (**Sup. Fig. 1B**), and alcian blue stain showed retention of submucosal glands and intact chondrocytes (**Sup. Fig. 1C**) in decellularized lung. Immunohistochemical staining similarly demonstrated the retention of basement membrane proteins collagen IV and laminin in decellularized lung (**Fig. 4E, iii-vi**). Methods to selectively target small airway segments are demonstrated on X-ray using a single customized dual occlusion catheter (**Fig. 4F, i**). The catheter is inserted into the targeted airway,

and the distal balloon is filled to occlusion. Then decellularization solution is instilled, and the proximal balloon is expanded. Additionally, the use of individually steerable micro occlusion catheters also allowed for directed therapeutic delivery while isolating proximal and/or distal areas during decellularization treatments (**Fig. 4F, ii**) and resulted in the removal of pseudostratified epithelium in targeted airways (**Fig. 4F, iii**).

Cell Delivery and Replacement in Human Lungs

Bronchoscopic cell delivery and the fundamental fluid mechanical forces acting on cells during deposition along the airway surface are shown schematically, where the hydrodynamic behaviors of cells delivered intratracheally are influenced by the viscous force (F_V), gravity (F_G), and the lift force (F_L) (**Fig. 5A,B**). A simplified force diagram of a spherical particle with diameter *d* can be applied to cells given their spherical shape following trypsinization and re-suspension. The buoyant force of the cell is negligible, as cell density is greater than that of the liquid. As the liquid plug travels through the airway, suspended cells carried by the liquid will be deposited onto the airway wall surface. Human mesenchymal stem cells (MSC) cultured *in vitro* (**Fig. 5C, i**) were labeled with quantum dots (**Fig. 5C, ii**) or CSFE (**Fig. 5C, iii**), re-suspended, and delivered bronchoscopically to targeted (non-decellularized) lung regions (**Fig. 5D**). A compact transpleural imaging system (**Fig. 5E, i**) enabled real-time, non-invasive imaging of delivered cells without the need for tissue biopsy. Labeled MSCs were visualized transpleurally immediately following delivery (**Fig. 5E, ii**) and were observed widely distributed throughout targeted regions of the distal lung. Post-procedural analysis of tissue sections confirmed homogenous distribution and attachment of MSCs throughout the distal lung (**Fig. 5F**) and within individual alveoli (**Fig. 5F, inset**). Movement of delivered cells into the interstitium (**Sup. Fig. 4A**) and co-expression with integrin β-1 (**Sup. Fig. 4B**) are suggestive of early engraftment.

Following decellularization, heterogeneous populations of pulmonary airway epithelial cells (AECs) were delivered using micro-volume delivery techniques previously described(20, 44). In larger proximal airways, a hydrogel comprised of lung extracellular matrix enriched in lung-specific basement membrane components was delivered prior to AECs to facilitate attachment and counteract the mechanical forces of gravity and ventilation. Post-procedural analysis demonstrated AECs lining larger airways (**Fig. 5G, i**) and distributed within alveoli in the distal lung (**Fig. 5G, ii**). Their topographic distribution was confirmed on histologic analysis (**Sup. Fig. 4C**), and co-staining with collagen IV (**Fig. 5H; Sup. Fig. 4D**) demonstrated the retention of a key basement membrane component following decellularization as well as the importance of extracellular matrix integrity for the attachment and integration of newly delivered cells.

Discussion

Worldwide the number of patients with end-stage lung disease continues to rise(45), and a viable alternative to traditional transplantation and donor lung utilization is desperately needed. Cellular therapeutics may play an important role in solving this problem, and the use of patient-derived cells circumvents many of the ethical and immunological issues related to allogeneic cell-based therapies.

Over the last decade, there have been significant advancements in two lung-related fields: *ex vivo* lung perfusion and lung bioengineering approaches based on the use of decellularized scaffolds.

Many groups have used the EVLP techniques and protocols pioneered by Steen and colleagues(46) and the Toronto group(24) to support, assess, and recover marginal quality donor lungs for transplantation(31, 47, 48). Meanwhile, the tools and methods for tissue decellularization and scaffold characterization (e.g., analysis of extracellular matrix components and biomechanics) has drastically improved(49, 50). However, the *de novo* bioengineering of functional human lungs suitable for transplantation remains challenging despite of advances in these technologies.

To address the challenges of whole organ bioengineering, we developed an approach to selectively target and intervene in specific lung regions. Cell replacement strategies targeting the treatment of only 20 – 25% may be sufficient to improve lung function and make an organ suitable for transplantation, or to reverse a specific disease phenotype. This approach addresses many of the challenges impeding current bioengineering efforts, including: (**i**) Scale: The human lung is comprised of roughly 2 x 10^{11} pneumocytes(51) and 75 x 10^{9} endothelial cells(52), with over 40 distinct cell phenotypes. Treating smaller lung volumes allows for the use of fewer cells and the selection of cell types most appropriate for targeted delivery locations. In addition, this addresses the practical challenges related to the maintenance, expansion, and tumor-forming potential of pluripotent cells during large-scale production(53). (**ii**) Blood gas barrier: Most decellularization approaches are perfusion-based and therefore necessitate recellularization of both the vascular and airway compartments. The vascular networks of the lung are among the most intricate in the human body. The integrity of this interface is vital to proper lung function and constitutes a major engineering hurdle. Our method of intratracheal decellularization preserves native lung vasculature and ensures that delivered cells are supplied with blood-based nutrients and factors necessary for engraftment and differentiation(54).

Our platform enabled delivery, visualization, and attachment of mesenchymal stem cells. Evidence suggests MSCs exert a variety of immunomodulatory effects and that the use of allogeneic MSCs is safe. We recognize the limitations of MSCs for recapitulating the normal cellular distribution of cell types within the lung, however they serve as an efficient and economical prototype for other cellular strategies, such iPS or distal basal cells(55-57). Additional studies are needed to determine optimal cell dosages, delivery route, and whether co-delivery with other cell types has benefit in the application of bioengineered constructs. Our regional decellularization technique resulted in the selective removal of the airway epithelium while preserving the pulmonary endothelium and extracellular matrix (**Fig. 4; Sup. Fig 1**). This approach resulted in the creation of a lung niche that supported the attachment of airway epithelial cells in proximal and distal airspaces (**Fig. 5; Sup. Fig. 4**). Targeted intervention into lobar and subsegmental regions as well as segments of proximal conducting airways was facilitated by the use of custom micro-catheters, trans-pleural imaging, lung extracellular matrix hydrogel, and balloon occlusion techniques – representing an integrated systems approach to tailored lung bioengineering. Aberrancy in airway epithelium has been linked to pathologic states of disease(58), and our understanding of disease pathogenesis and cellular derangement continues to improve. Further refinements in these techniques and devices will allow for more localized targeting, and more sophisticated decellularization agents (e.g., toxin-linked or antibody-mediated) may enable the highly selective removal and subsequent replacement of specific cell types.

This study was designed and limited to serve as an initial proof-of-concept to demonstrate the feasibility of targeted decellularization and recellularization in extracorporeal lungs. There are several limitations to the current study: (***i***) While techniques and cell interventions were being refined, investigations into lung function and gas exchange did not take place, as our EVLP system was based on acellular perfusate and mechanics was not the focus of this study. (***ii***) Cell-level

analysis such as gene expression and ability to observe differentiation was not conducted, given the relatively short duration of time lungs were maintained on *ex vivo* support. Currently, this is a major limitation in the field and further cell delivery studies are planned utilizing our cross-circulation platform for prolonged normothermic support in order to study cell replacement therapy over the course of days.

Continued advancement in the field of human lung bioengineering will require improved physiologic and biochemical assessment of donor lungs. Currently, there is no standardized reporting of donor characteristics, and the reasons lungs are not transplantable are often multi-factorial; thus, the true incidence of specific pathology is difficult to determine. Biochemical markers of alveolar epithelial barrier dysfunction(59), donor exosome profiles(60), and detailed cytokine analyses(61) of donor lungs may improve donor-recipient matching, enable better prediction of outcomes, and help identify lungs most amenable to cell replacement therapy in the future.

Conclusions

In this study, we demonstrated that the utilization of human lungs unsuitable for transplantation and supported by EVLP allowed for the development and refinement of (***i***) an integrated lung support platform with advanced theranostics, (***ii***) selective removal of native lung epithelium, (***iii***) maintenance of extracellular matrix components essential for providing the biophysical and biochemical cues to therapeutic replacement cells, and (***iv***) the effective delivery and attachment of therapeutic cells (MSCs, AECs) into targeted lung regions. These results suggest that targeted cell

replacement in extracorporeal organs is feasible and may ultimately lead to chimeric organs suitable for transplantation. Furthermore, as mechanisms for somatic reprogramming and genetic manipulation of patient-specific cell lines advances, this work may have profound translational application in patients during early *in situ* interventions to halt or reverse disease trajectory (**Fig. 1B**), and ultimately preclude the need for transplantation altogether.

DATA AVAILABILITY

The authors declare that all data supporting the findings of this study are available within the paper or online supplement.

ACKNOWLEDGEMENTS

The authors would like to thank S. Halligan and K. Cunningham for administrative and logistical support; H. Wobma for providing mesenchymal cells; L. Cohen-Gould for TEM imaging; the Herbert Irving Comprehensive Cancer Center Molecular Pathology Shared Resources, including T. Wu, D. Sun, R. Chen for help with analytics.

COMPETING FINANCIAL INTERESTS

The authors declare no competing financial interests.

AUTHOR CONTRIBUTIONS

B.A.G., J.D.O., J.K., K.F., and M.B. performed experiments. B.A.G., J.D.O., M.B., and G.V.-N. co-analyzed data, co-wrote manuscript.

AUTHOR DISCLOSURES

None

SOURCES OF FUNDING

The authors gratefully acknowledge funding support from the National Institutes of Health (grants HL134760, EB002520, HL007854), the Rick Bartlett Memorial Foundation, and the Mikati Foundation.

REFERENCES

1. Cypel M, Keshavjee S: Extending the donor pool: rehabilitation of poor organs. Thoracic surgery clinics 2015;25:27-33.

2. Elgharably H, Shafii AE, Mason DP: Expanding the Donor Pool: Donation After Cardiac Death. Thoracic surgery clinics 2015;25:35-46.

3. Botha P, Trivedi D, Weir CJ, et al.: Extended donor criteria in lung transplantation: impact on organ allocation. The Journal of thoracic and cardiovascular surgery 2006;131:1154-60.

4. Valapour M, Skeans M, Heubner B, et al.: OPTN/SRTR 2013 annual data report: lung. American Journal of Transplantation 2015;15:1-28.

5. Wagner DE, Bonvillain RW, Jensen T, et al.: Can stem cells be used to generate new lungs? Ex vivo lung bioengineering with decellularized whole lung scaffolds. Respirology 2013;18:895-911.

6. Ochs M, Nyengaard JR, Jung A, et al.: The number of alveoli in the human lung. American journal of respiratory and critical care medicine 2004;169:120-4.

7. Ott HC, Clippinger B, Conrad C, et al.: Regeneration and orthotopic transplantation of a bioartificial lung. Nat Med 2010;16:927-33.

8. Petersen TH, Calle EA, Zhao L, et al.: Tissue-engineered lungs for in vivo implantation. Science 2010;329:538-41.

9. Gilpin SE, Guyette JP, Gonzalez G, et al.: Perfusion decellularization of human and porcine lungs: bringing the matrix to clinical scale. The Journal of Heart and Lung Transplantation 2014;33:298-308.

10. Wagner DE, Bonenfant NR, Sokocevic D, et al.: Three-dimensional scaffolds of acellular human and porcine lungs for high throughput studies of lung disease and regeneration. Biomaterials 2014;35:2664-79.

11. Aggarwal S, Pittenger MF: Human mesenchymal stem cells modulate allogeneic immune cell responses. Blood 2005;105:1815-22.

12. Ortiz LA, DuTreil M, Fattman C, et al.: Interleukin 1 receptor antagonist mediates the antiinflammatory and antifibrotic effect of mesenchymal stem cells during lung injury. Proceedings of the National Academy of Sciences 2007;104:11002-7.

13. Wobma HM, Liu D, Vunjak-Novakovic G: Paracrine Effects of Mesenchymal Stromal Cells Cultured in Three-Dimensional Settings on Tissue Repair. ACS Biomaterials Science & Engineering 2017.

14. Islam MN, Das SR, Emin MT, et al.: Mitochondrial transfer from bone-marrow-derived stromal cells to pulmonary alveoli protects against acute lung injury. Nature medicine 2012;18:759-65.

15. Takahashi K, Yamanaka S: Induction of pluripotent stem cells from mouse embryonic and adult fibroblast cultures by defined factors. cell 2006;126:663-76.

16. Fitzhugh CD, Hsieh MM, Cordes S, et al.: At Least 20% Donor Myeloid Chimerism Is Necessary to Reverse the Sickle Phenotype after Allogeneic Hematopoietic Stem Cell Transplantation. Am Soc Hematology; 2016.

17. Walters M, Patience M, Leisenring W, et al.: Stable mixed hematopoietic chimerism after bone marrow transplantation for sickle cell anemia. Biology of Blood and Marrow Transplantation 2001;7:665-73.

18. Johnson LG, Olsen JC, Sarkadi B, Moore KL, Swanstrom R, Boucher RC: Efficiency of gene transfer for restoration of normal airway epithelial function in cystic fibrosis. Nature genetics 1992;2:21-5.

19. Ramalho AS, Beck S, Meyer M, Penque D, Cutting GR, Amaral MD: Five percent of normal cystic fibrosis transmembrane conductance regulator mRNA ameliorates the severity of pulmonary disease in cystic fibrosis. American journal of respiratory cell and molecular biology 2002;27:619-27.

20. Kim J, O'Neill JD, Dorrello NV, Bacchetta M, Vunjak-Novakovic G: Targeted delivery of liquid microvolumes into the lung. Proceedings of the National Academy of Sciences 2015;112:11530-5.

21. Saxena P, Zimmet AD, Snell G, Levvey B, Marasco SF, McGiffin DC: Procurement of lungs for transplantation following donation after circulatory death: the Alfred technique. Journal of Surgical Research 2014;192:642-6.

22. Sundaresan S, Trachiotis GD, Aoe M, Patterson GA, Cooper JD: Donor lung procurement: assessment and operative technique. The Annals of thoracic surgery 1993;56:1409-13.

23. O'Neill JD, Guenthart BA, Kim J, et al.: Cross-circulation for extracorporeal support and recovery of the lung. Nature Biomedical Engineering 2017;1:0037.

24. Cypel M, Yeung JC, Hirayama S, et al.: Technique for prolonged normothermic ex vivo lung perfusion. The Journal of Heart and Lung Transplantation 2008;27:1319-25.

25. O'Neill JD, Anfang R, Anandappa A, et al.: Decellularization of human and porcine lung tissues for pulmonary tissue engineering. The Annals of thoracic surgery 2013;96:1046-56.

26. Cypel M, Liu M, Rubacha M, et al.: Functional repair of human donor lungs by IL-10 gene therapy. Science translational medicine 2009;1:4ra9-4ra9.

27. Wierup P, Haraldsson Å, Nilsson F, et al.: Ex vivo evaluation of nonacceptable donor lungs. The Annals of thoracic surgery 2006;81:460-6.

28. Egan TM, Haithcock JA, Nicotra WA, et al.: Ex vivo evaluation of human lungs for transplant suitability. The Annals of thoracic surgery 2006;81:1205-13.

29. Ingemansson R, Eyjolfsson A, Mared L, et al.: Clinical transplantation of initially rejected donor lungs after reconditioning ex vivo. The Annals of thoracic surgery 2009;87:255-60.

30. Ware LB, Wang Y, Fang X, et al.: Assessment of lungs rejected for transplantation and implications for donor selection. The Lancet 2002;360:619-20.

31. Wallinder A, Ricksten S-E, Hansson C, et al.: Transplantation of initially rejected donor lungs after ex vivo lung perfusion. The Journal of thoracic and cardiovascular surgery 2012;144:1222-8.

32. Pêgo-Fernandes P, de Medeiros I, Mariani A, et al.: Ex vivo lung perfusion: early report of Brazilian experience. Transplantation proceedings: Elsevier; 2010. p. 440-3.

33. Boffini M, Ricci D, Barbero C, et al.: Ex vivo lung perfusion increases the pool of lung grafts: analysis of its potential and real impact on a lung transplant program. Transplantation proceedings: Elsevier; 2013. p. 2624-6.

34. Ware LB, Fang X, Wang Y, Babcock WD, Jones K, Matthay MA: High prevalence of pulmonary arterial thrombi in donor lungs rejected for transplantation. The Journal of heart and lung transplantation 2005;24:1650-6.

35. Medeiros IL, Pêgo-Fernandes PM, Mariani AW, et al.: Histologic and functional evaluation of lungs reconditioned by ex vivo lung perfusion. The Journal of Heart and Lung Transplantation 2012;31:305-9.

36. Andreasson A, Karamanou DM, Perry JD, et al.: The effect of ex vivo lung perfusion on microbial load in human donor lungs. The Journal of Heart and Lung Transplantation 2014;33:910-6.

37. Mariani AW, Medeiros IL, Pego-Fernandes PM, et al.: Cold ischemia or topical-ECMO for lung preservation: a randomized experimental study. Sao Paulo Medical Journal 2014;132:28-35.

38. Lee JW, Fang X, Gupta N, Serikov V, Matthay MA: Allogeneic human mesenchymal stem cells for treatment of E. coli endotoxin-induced acute lung injury in the ex vivo perfused human lung. Proceedings of the National Academy of Sciences 2009;106:16357-62.

39. La Francesca S, Ting AE, Sakamoto J, et al.: Multipotent adult progenitor cells decrease cold ischemic injury in ex vivo perfused human lungs: an initial pilot and feasibility study. Transplantation research 2014;3:19.

40. Wallinder A, Ricksten S-E, Silverborn M, et al.: Early results in transplantation of initially rejected donor lungs after ex vivo lung perfusion: a case–control study. European Journal of Cardio-Thoracic Surgery 2014;45:40-5.

41. McAuley DF, Curley GF, Hamid UI, et al.: Clinical grade allogeneic human mesenchymal stem cells restore alveolar fluid clearance in human lungs rejected for transplantation. American Journal of Physiology-Lung Cellular and Molecular Physiology 2014;306:L809-L15.

42. McElhinney DB, Khan JH, Babcock WD, Hall TS: Thoracic organ donor characteristics associated with successful lung procurement. Clinical transplantation 2001;15:68-71.

43. George TJ, Arnaoutakis GJ, Beaty CA, et al.: A physiologic and biochemical profile of clinically rejected lungs on a normothermic ex vivo lung perfusion platform. Journal of Surgical Research 2013;183:75-83.

44. Kim J, Guenthart B, O'Neill JD, Dorrello NV, Bacchetta M, Vunjak-Novakovic G: Controlled delivery and minimally invasive imaging of stem cells in the lung. Scientific Reports 2017;7.

45. Marciniuk D, Ferkol T, Nana A, et al.: Respiratory diseases in the world. Realities of today–opportunities for tomorrow. African Journal of Respiratory Medicine Vol 2014;9.

46. Steen S, Sjoberg T, Pierre L, Liao Q, Eriksson L, Algotsson L: Transplantation of lungs from a non-heart-beating donor. Lancet 2001;357:825-9.

47. Cypel M, Yeung JC, Liu M, et al.: Normothermic ex vivo lung perfusion in clinical lung transplantation. New England Journal of Medicine 2011;364:1431-40.

48. Zych B, Popov AF, Stavri G, et al.: Early outcomes of bilateral sequential single lung transplantation after ex-vivo lung evaluation and reconditioning. The Journal of Heart and Lung Transplantation 2012;31:274-81.

49. Wobma H, Vunjak-Novakovic G: Tissue engineering and regenerative medicine 2015: a year in review. Tissue Engineering Part B: Reviews 2016;22:101-13.

50. Gilpin SE, Ott HC: Using nature's platform to engineer bio-artificial lungs. Annals of the American Thoracic Society 2015;12:S45-S9.

51. Mercer RR, Russell ML, Roggli VL, Crapo JD: Cell number and distribution in human and rat airways. American journal of respiratory cell and molecular biology 1994;10:613-24.

52. Stone KC, Mercer RR, Freeman BA, Chang L-Y, Crapo JD: Distribution of lung cell numbers and volumes between alveolar and nonalveolar tissue. American Review of Respiratory Disease 1992;146:454-6.

53. Fox IJ, Daley GQ, Goldman SA, Huard J, Kamp TJ, Trucco M: Use of differentiated pluripotent stem cells in replacement therapy for treating disease. Science 2014;345:1247391.

54. Dorrello NV, Guenthart BA, O'Neill JD, et al.: Functional vascularized lung grafts for lung bioengineering. Science Advances 2017;3:e1700521.

55. Huang SX, Green MD, de Carvalho AT, et al.: The in vitro generation of lung and airway progenitor cells from human pluripotent stem cells. Nature protocols 2015;10:413-25.

56. Huang SX, Islam MN, O'Neill J, et al.: Efficient generation of lung and airway epithelial cells from human pluripotent stem cells. Nat Biotechnol 2014;32:84-91.

57. Chen Y-W, Huang SX, de Carvalho ALRT, et al.: A three-dimensional model of human lung development and disease from pluripotent stem cells. Nature cell biology 2017;19:542.

58. Zemans RL, Matthay MA: Bench-to-bedside review: the role of the alveolar epithelium in the resolution of pulmonary edema in acute lung injury. Critical Care 2004;8:469.

59. Frank JA, Briot R, Lee JW, Ishizaka A, Uchida T, Matthay MA: Physiological and biochemical markers of alveolar epithelial barrier dysfunction in perfused human lungs. American Journal of Physiology-Lung Cellular and Molecular Physiology 2007;293:L52-L9.

60. Gunasekaran M, Xu Z, Nayak D, et al.: Donor‐Derived Exosomes With Lung Self‐Antigens in Human Lung Allograft Rejection. American Journal of Transplantation 2016.

61. Kaneda H, Waddell T, De Perrot M, et al.: Pre‐Implantation Multiple Cytokine mRNA Expression Analysis of Donor Lung Grafts Predicts Survival After Lung Transplantation in Humans. American journal of transplantation 2006;6:544-51.

FIGURE CAPTIONS

Figure 1 | Cell replacement in *ex vivo* lung bioengineering and envisioned *in situ* application. (**A**) *Ex vivo lung* bioengineering and cell replacement strategy to recover lungs unsuitable for transplantation. (i) Schematic showing human lungs procured and placed on ex vivo support enabling regional cell replacement and creation of functionally improved chimeric lungs. (ii). Schematic showing the selective removal of respiratory epithelium with preservation of native lung and extracellular matrix components followed by therapeutic cell delivery, attachment, and differentiation. (iii) Additional diagnostic and therapeutic interventions enabled by *ex vivo lung*

perfusion and prolonged extracorporeal support. (**B**) Envisioned *in situ* cell replacement in patients with lung injury or disease. Collection of patient's own cells (1). Somatic reprogramming and genetic modification of patient-derived cells to obtain healthy patient-specific progenitor cells (iPSC) (2). Delivery of healthy progenitors into targeted lung regions in damaged lungs to treat or reverse the trajectory of disease (3).

Figure 2 | *Ex vivo* lung perfusion (EVLP) equipment and setup. (**A**) Perfusion cart and organ preservation stand housing perfusion, ventilation, and imaging equipment for the extracorporeal lung. (**B**) EVLP circuit diagram with integrated circuit elements. A, airflow probe; H, heat exchanger; HC, humidified chamber; P, pressure sensor; PA, pulmonary artery; PV, pulmonary vein; Q, flow probe; T, temperature probe; WB, warm organ basin. $\Delta h_{reservoir}$ = ± 45 cm, Δh_{lung} = ± 32 cm. (**C**) Flow (L/min) within PA and PV cannulas of extracorporeal lung (n = 6). (**D**) Trans-pulmonary gradient (TPG), the difference between PA and PV pressures (n = 6). All values represent mean ± standard deviation.

Figure 3 | Donor lung cannulation techniques and donor lung characteristics. (**A**) (i) Left atrial cuff after removal of the heart allowing visualization of pulmonary veins (arrow heads). T, trachea. PA, pulmonary artery. (ii) Dissected human aortic arch used for cannulation and serving as a bio-bridge in the management of pulomary venous drainage. DA, descending aorta. IA, innominate artery. LSC, left subclavian artery. LCC, left common carotid artery. RCC, right common carotid artery. RSC, right subclavian artery Lung cannulation with the aortic arch (AA) serving as a bio-bridge and a portion of descending arota serving as a graft to facilitate the insertion of pulmonary venous (PV) and arterial (PA) cannulas. Endotracheal tube (ETT) secured within the trachea (iii). (**B**) Donor tissue options for use as a bio-bridge. (i) Aortic arch, (ii) abdominal aorta, (iii)

pericardium. (iv) Cannulation of lungs using aortic arch or (v) pericardium. (**C**) Imaging examples of lungs unsuitable for transplantation prior to procurement. (i) Computed tomography (CT) scan of chest demonstrating collapse/consolidation of the right lower lobe and left lower lobe base, and (ii) chest X-ray (CXR) with opacity/atelectasis of the right lower lobe. (iii, iv) Gross appearance of unsuitable lungs and (v, vi) bronchoscopic view of the airway demonstrating inflammation and removal of a mucous plug, respectively. (**D**) Gross appearance (i) and thermography (ii) of human lungs following procurment, cold flush, and placement within warm organ basin. (**E**) Periodic acid-Schiff (PAS) stain of bronchoalveolar lavage fluid obtained immediately after human lung procurement. (**F**) Delivery and uptake of cell viability marker (CFSE) by alveolar cells in the distal lung of unsuitable human donor lungs.

Figure 4 | Human lung decellularization, extracellular matrix preservation, and targeted therapeutic approach. (**A**) Schematic of lung decellularization demonstrating removal of lung epithelium with preservation of the basement membrane (BM) and extracellular matrix (ECM). (**B**) Regional decellularization of the lung (blue dye added for visualization). (i) Bronchoscopic view and (ii) gross appearance following delivery into the lateral segment of the right middle lobe. (**C**) Histologic comparison of native and de-epithelialized lung. (i-iii) H&E of native lung and (iv-vi) decellularized lung demonstrating removal of lung epithelium (arrows). (**D**) Transmission electron microscopy (TEM) of native lung demonstrating intact blood-gas barrier with type II cell (arrow), and decellularized lung with removal of type I pneumocyte cell membranes, exposure of the basement membrane, detached type II cell (arrow), and intact endothelial cell (star). (**E**) Retention of extracellular matrix components. (i-ii) Trichrome staining showing retention of collagen (blue) and elastic fibers (purple) surrounding airways and vessels (stars) with removal of airway epithelium (arrows). (iii-vi) Collagen IV and laminin immunostaining in native and decellularized lung. (**F**) Targeted lung decellularizaiton methods. (i) Xray imaging showing a double balloon

occlusion catheter system to treat segments of proximal conducting airways. Treatment area highlighted in blue and marked by arrow. (ii) Dual catheter use to occlude one lung segment (arrow) while treating or also occluding more distal lung (star). (iii) Histologic analysis of large airway following treatment demonstrating removal of pseudostratisfied columnar epithelium (arrows).

Figure 5 | Cell replacement in human lungs. (**A**) Targeted intratracheal cell delivery and deposition onto airway surfaces. (**B**) Cell deposition by microvolume liquid plug delivery. Hydrodynamic motion of cells influenced by internal circulatory flow patterns and forces F_L (lift), F_V (viscous), F_G (gravity). (**C**) Human MSCs (i) cultured *in vitro* and labeled with (ii) quantum dots (Qdot) or (iii) CSFE. (**D**) X-ray image during bronchoscopic delivery (arrow marks distal tip). (**E**) (i) Transpleural imaging camera used to confirm the (ii) delivery and distrubution of delivered cells. (**F**) Histologic analysis of delivered MSCs. Global distribution and in a single alveolus (inset). (**G**) Cell replacement by targeted delivery of airway epithelial cells (AEC) following decellularization. (**H**) Collagen IV immunostaining highlighting retention of a key extracellular matrix component critical for the attachment of cells to the basement membrane. Delivered cells (MSCs, AECs) demonstrate flattening and morphological adaptations to surrounding alveoli.

TABLE 1

Table 1 Characteristics of Donors with Lungs Deemed Unsuitable for Transplantation (*n* = 756)

Age (yrs)	45.7 ± 6.9
(*n* = 432)	
Gender	
(*n* = 709)	
Male	424 (59.8%)
Female	285 (40.2%)
Cause of Brain Death	
(*n* = 301)	
Trauma	171 (56.8%)
Intracerebral Hemorrhage	103 (34.2%)
Other	27 (8.9%)
Presence of Underlying Lung Disease	40 (6.9%)
(*n* = 579)	
Smoking History (> 20 pack years)	142 (23.1%)
(*n* = 616)	
P/F Ratio (mmHg)	259.18 ± 66.92
(*n* = 233)	

PaO_2 on 100% FiO_2 (mmHg) (n = 49)	236.17 ± 101.26
Abnormal CXR (edema or infiltrates) (n = 411)	150 (36.5%)
Suspected PNA or Aspiration (n = 491)	130 (26.5%)
Time on Ventilator (hrs) (n = 51)	108.7 ± 47.1
Time from Brain Death to Procurement (hrs) (n = 192)	36.65 ± 14.64

Data represent combined analyses from 18 peer-reviewed reports in the literature. The number of donors (n) reported in each category is listed in the left column underneath each category. Values for each category represent mean ± SD or n (%).

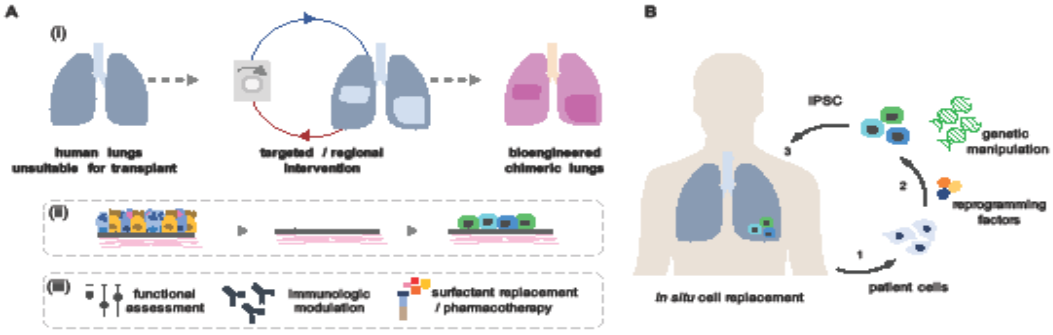

Figure 1 | Cell replacement in *ex vivo* lung bioengineering and envisioned *in situ* application. **(A)** *Ex vivo lung* bioengineering and cell replacement strategy to recover lungs unsuitable for transplantation. **(I)** Schematic showing human lungs procured and placed on ex vivo support enabling regional cell replacement and creation of functionally improved chimeric lungs. **(II)**. Schematic showing the selective removal of respiratory epithelium with preservation of native lung and extracellular matrix components followed by therapeutic cell delivery, attachment, and differentiation. **(III)** Additional diagnostic and therapeutic interventions enabled by *ex vivo lung* perfusion and prolonged extracorporeal support. **(B)** Envisioned *in situ* cell replacement in patients with lung injury or disease. Collection of patient's own cells (1). Somatic reprogramming and genetic modification of patient-derived cells to obtain healthy patient-specific progenitor cells (iPSC) (2). Delivery of healthy progenitors into targeted lung regions in damaged lungs to treat or reverse the trajectory of disease (3).

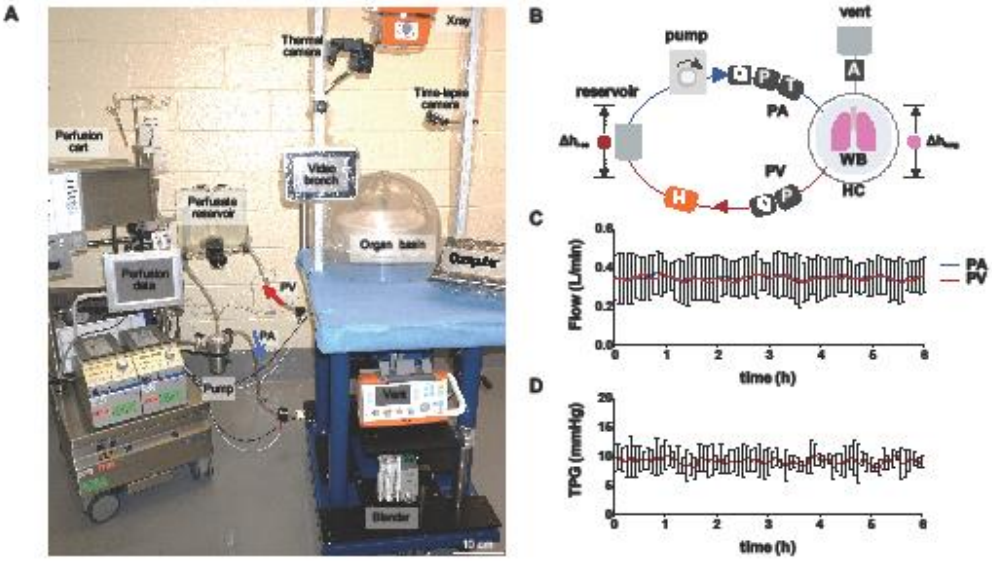

Figure 2 | *Ex vivo* lung perfusion (EVLP) equipment and setup. (**A**) Perfusion cart and organ preservation stand housing perfusion, ventilation, and imaging equipment for the extracorporeal lung. (**B**) EVLP circuit diagram with integrated circuit elements. A, airflow probe; H, heat exchanger; HC, humidified chamber; P, pressure sensor; PA, pulmonary artery; PV, pulmonary vein; Q, flow probe; T, temperature probe; WB, warm organ basin. $\Delta h_{reservoir} = \pm 45$ cm, $\Delta h_{lung} = \pm 32$ cm. (**C**) Flow (L/min) within PA and PV cannulas of extracorporeal lung ($n = 6$). (**D**) Trans-pulmonary gradient (TPG), the difference between PA and PV pressures ($n = 6$). All values represent mean ± standard deviation.

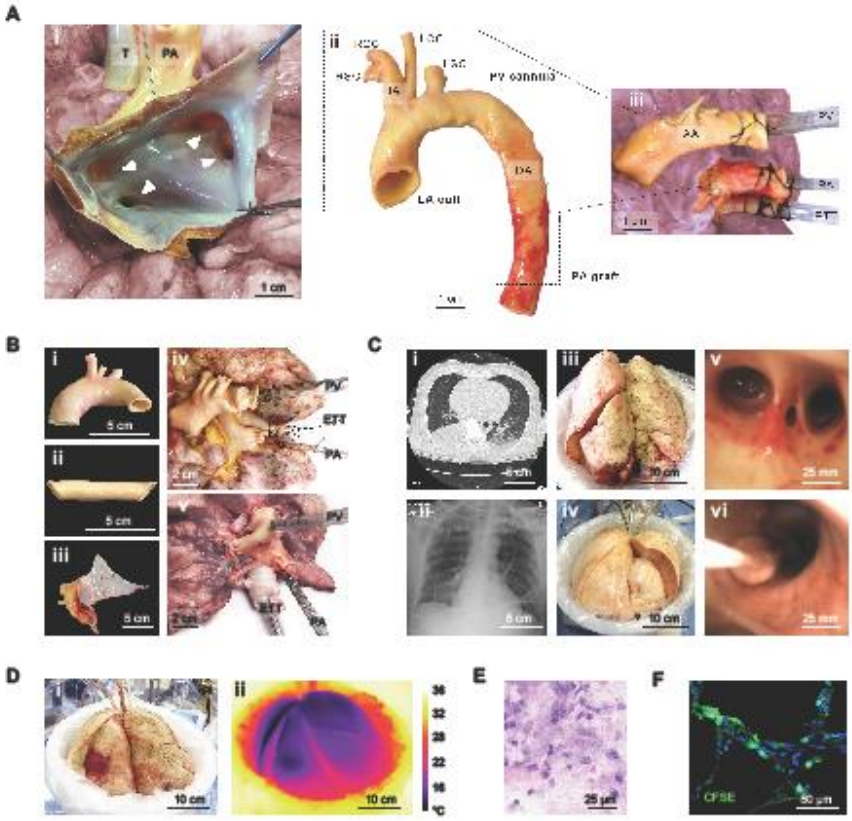

Figure 3 | Donor lung cannulation techniques and donor lung characteristics. (A) (i) Left atrial cuff after removal of the heart allowing visualization of pulmonary veins (arrow heads). T, trachea. PA, pulmonary artery. (ii) Dissected human aortic arch used for cannulation and serving as a bio-bridge in the management of pulmary venous drainage. DA, descending aorta. IA, innominate artery. LSC, left subclavian artery. LCC, left common carotid artery. RCC, right common carotid artery. RSC, right subclavian artery Lung cannulation with the aortic arch (AA) serving as a bio-bridge and a portion of descending arota serving as a graft to facilitate the insertion of pulmonary venous (PV) and arterial (PA) cannulas. Endotracheal tube (ETT) secured within the trachea (iii). (B) Donor tissue options for use as a bio-bridge. (i) Aortic arch, (ii) abdominal aorta, (iii) pericardium. (iv) Cannulation of lungs using aortic arch or (v) pericardium. (C) Imaging examples of lungs unsuitable for transplantation prior to procurement. (i) Computed tomography (CT) scan of chest demonstrating collapse/consolidation of the right lower lobe and left lower lobe base, and (ii) chest X-ray (CXR) with opacity/atelectasis of the right lower lobe. (iii, iv) Gross appearance of unsuitable lungs and (v, vi) bronchoscopic view of the airway demonstrating inflammation and removal of a mucous plug, respectively. (D) Gross appearance (i) and thermography (ii) of human lungs following procurment, cold flush, and placement within warm organ basin. (E) Periodic acid-Schiff (PAS) stain of bronchoalveolar lavage fluid obtained immediately after human lung procurement. (F) Delivery and uptake of cell viability marker (CFSE) by alveolar cells in the distal lung of unsuitable human donor lungs.

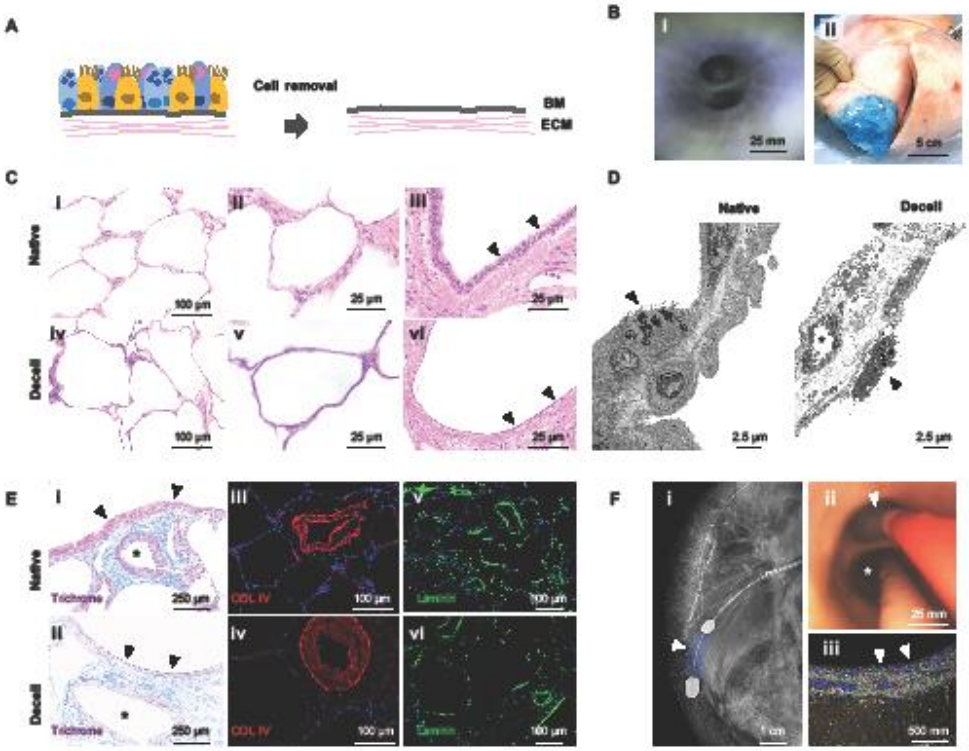

Figure 4 | Human lung decellularization, extracellular matrix preservation, and targeted therapeutic approach. (A) Schematic of lung decellularization demonstrating removal of lung epithelium with preservation of the basement membrane (BM) and extracellular matrix (ECM). (B) Regional decellularization of the lung (blue dye added for visualization). (I) Bronchoscopic view and (II) gross appearance following delivery into the lateral segment of the right middle lobe. (C) Histologic comparison of native and de-epithelialized lung. (I-III) H&E of native lung and (Iv-vI) decellularized lung demonstrating removal of lung epithelium (arrows). (D) Transmission electron microscopy (TEM) of native lung demonstrating intact blood-gas barrier with type II cell (arrow), and decellularized lung with removal of type I pneumocyte cell membranes, exposure of the basement membrane, detached type II cell (arrow), and intact endothelial cell (star). (E) Retention of extracellular matrix components. (I-II) Trichrome staining showing retention of collagen (blue) and elastic fibers (purple) surrounding airways and vessels (stars) with removal of airway epithelium (arrows). (III-vI) Collagen IV and laminin immunostaining in native and decellularized lung. (F) Targeted lung decellularizaiton methods. (I) Xray imaging showing a double balloon occlusion catheter system to treat segments of proximal conducting airways. Treatment area highlighted in blue and marked by arrow. (II) Dual catheter use to occlude one lung segment (arrow) while treating or also occluding more distal lung (star). (III) Histologic analysis of large airway following treatment demonstrating removal of pseudostratisfied columnar epithelium (arrows).

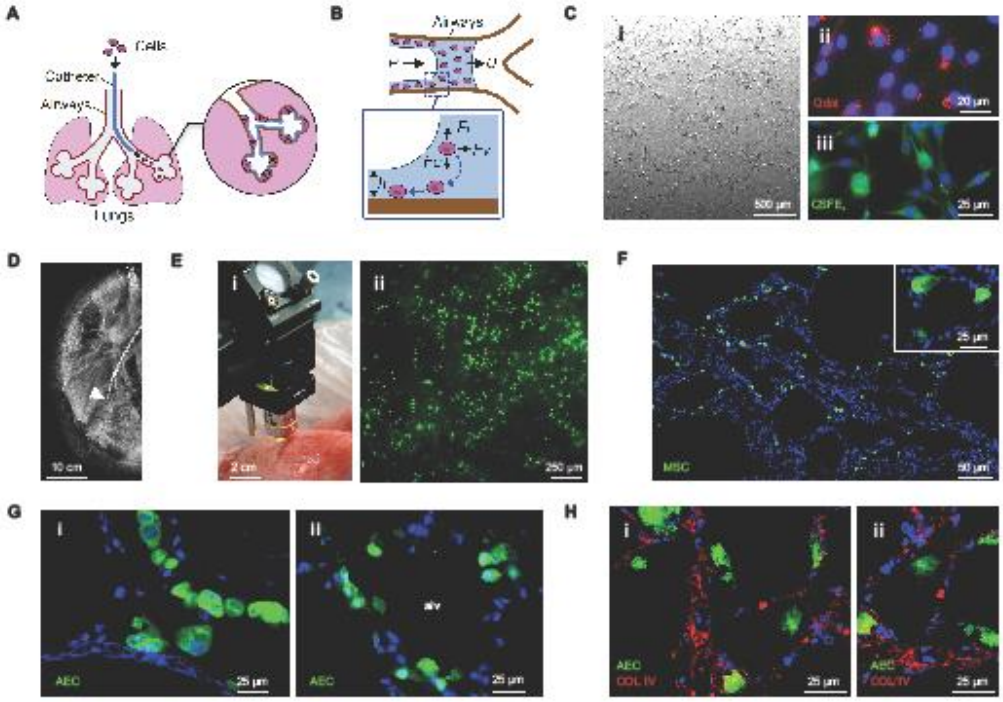

Figure 5 | Cell replacement in human lungs. (**A**) Targeted intratracheal cell delivery and deposition onto airway surfaces. (**B**) Cell deposition by microvolume liquid plug delivery. Hydrodynamic motion of cells influenced by internal circulatory flow patterns and forces F_L (lift), F_V (viscous), F_G (gravity). (**C**) Human MSCs (**I**) cultured *in vitro* and labeled with (**II**) quantum dots (Qdot) or (**III**) CSFE. (**D**) X-ray image during bronchoscopic delivery (arrow marks distal tip). (**E**) (**I**) Transpleural imaging camera used to confirm the (**II**) delivery and distrubution of delivered cells. (**F**) Histologic analysis of delivered MSCs. Global distribution and in a single alveolus (inset). (**G**) Cell replacement by targeted delivery of airway epithelial cells (AEC) following decellularization. (**H**) Collagen IV immunostaining highlighting retention of a key extracellular matrix component critical for the attachment of cells to the basement membrane.